CLM-P680

CLM-P680

UKAEA

Preprint

THE 1-D SIMULATION OF DITE NEUTRAL INJECTION HEATING EXPERIMENTS

R. D. GILL
G. D. KERBEL
A. A. MIRIN

CULHAM LABORATORY
Abingdon Oxfordshire

1982

CLM-P680

THE 1-D SIMULATION OF DITE NEUTRAL INJECTION HEATING EXPERIMENTS

R.D. Gill, G.D. Kerbel* and A.A. Mirin*

Culham Laboratory, Abingdon, Oxon., OX14 3DB, UK
(Euratom/UKAEA Fusion Association)

ABSTRACT

A non-linear time dependent Fokker-Planck transport code is used to simulate neutral beam injection experiments, without the divertor, in the DITE tokamak. Injection of H^{o} into both D^{+} and H^{+} plasmas is considered. The effects of both high and low Z impurities are modelled. The effect of beam impurity charge exchange on the radiative power loss is modelled. Transverse conductivities and diffusivities are derived which best represent the experimental data, both with and without injection, for six well documented experiments. Good overall agreement is obtained.

*National Magnetic Fusion Energy Computer Centre,
Lawrence Livermore National Laboratory,
Livermore, CA 94550, USA.

To be submitted to Plasma Physics

March 1982

1. INTRODUCTION

The original aim of 1-D radial transport calculations for tokamaks was to reproduce the tokamak behaviour from an entirely theoretical point of view. Both the set of equations and the transport coefficients were to be supplied by the theory. In early work[1] the transport coefficients were calculated assuming that the plasma was in the banana regime of collisionality and included mass transport and neutral gas input. Calculations were also done with a simplified three regime thermal transport model without mass transport and a two regime model with enhanced mass transport[2]. This approach was subsequently improved upon to produce the six regime model of plasma transport[3]. However, despite some of the successes of this approach, because of the poorly understood nature of the electron thermal conductivity and the diffusion coefficient, the use of theoretical transport coefficients became supplemented by an empirical approach in which the coefficients were chosen to give reasonable overall agreement with experimentally determined quantities, and this is the approach of this paper.

In injection heated discharges it was also necessary to simulate the behaviour of the hot injected ions. The necessary theoretical technique was originally developed to study beam heated mirror confined plasmas and was extended to apply to tokamak injection heated discharges. A fully non-linear Fokker-Planck transport code[4,5] was applied to the study of various beam driven tokamak fusion reactors in which there were several energy components of the fast ions, to the prediction of the behaviour of PDX[6] and TFTR[7], and to the analysis of the neutron emission from the neutral beam heated discharges in PLT[8].

It is the intention of the present paper to report the results of simulation studies for DITE carried out using this non-linear Fokker-Planck/Transport code with empirical transport coefficients. The DITE machine is heated by high power (~ 1MW) neutral injection beams so that this approach should be particularly appropriate. A set of experiments with a variety of machine parameters is chosen and time dependent simulations using a single set of transport coefficients for all the data is carried out. Reasonable overall agreement is found both for the magnitude and time dependence of the measured quantities.

One of the difficulties encountered by all simulation models of the sort described here is their inability to model the tokamak start up. In some models there arises a large current skin effect which is not observed experimentally[9]. Therefore no attempt will be made to model the start up phase of the discharge. Instead, the plasma behaviour is simulated starting from predetermined profiles of density and temperature, at a time well after the initiation of the discharge.

2. THEORETICAL MODEL

All the calculations reported in this paper are carried out using the 1-D non-linear Fokker-Planck/Transport code developed by Mirin et.al.[5] who give the equations which define the model and describe their method of solution. Here we list the major features of the model and write down the transport equations as it is these in which we are particularly interested.

The model allows for four classes of particles: fast injected ions, plasma ions, electrons and neutrals. The injected ions are

described by non-linear Fokker-Planck equations which include collisions with all charged species at each radial position. The effects of charge exchange, deceleration, orbit losses and the electric field are all included. The initial trapping and deposition of the fast ions is determined with a Monte-Carlo code[10] which includes finite injector geometry. It is assumed thereafter that particles remain on the flux surfaces on which they were born and that there is no radial diffusion of the fast ions. There are several energy components in the injected species (with maximum energy E) and for DITE the power ratios have been measured[11] as $P(E) : P(E/2) : P(E/3) = 77 : 18 : 5$.

The plasma ions are described by radial transport equations with empirical or neoclassical conduction coefficients. The energy sources and sinks include beam and ohmic heating, ionisation and charge exchange. The equation for the ions is:

$$\frac{\partial}{\partial t}\left(\frac{3}{2}\sum_a n_a T_i\right) = -\frac{1}{r}\frac{\partial}{\partial r}\left(r\left(\frac{5}{2}T_i\sum_a \Gamma_a + K_i\sum_a n_a\frac{\partial T_i}{\partial r}\right)\right)$$

Convection — Conduction

$$+\sum_a Q_{ab} + \sum_{a,b}\int S_{bc}\,E_{bc}\,d\vec{v}\,\delta(a,b) + \sum_a S_{ai}\,\tilde{E}_a$$

Heating of plasma by energetic particles — Energy gained when energetic particles become plasma particles — Energy gained due to ionisation of neutrals

$$+ W_{cx} + Q_\Delta \qquad \ldots (1)$$

Energy gained due to charge exchange — Heat transfer between electrons and plasma ions

where n and T are the density and temperature and the different source terms are identified. The different plasma ion species, all assumed to be at a common temperature, are denoted by subscript 'a'; $\tilde{E}_a$ is the energy of the neutrals; and K_i is the ion thermal conductivity.

A similar equation describes the radial energy transport of the electrons:

$$\frac{\partial}{\partial t}\left(\frac{3}{2} n_e T_e\right) = -\frac{1}{r}\frac{\partial}{\partial r}\left(r\left(\frac{5}{2} T_e \sum_a Z_a \Gamma_a + K_e n_e \frac{\partial T_e}{\partial r}\right)\right)$$

Convection | Conduction

$$+ Q_{eb} - Q_r - Q_\Delta + j_\Phi E_\Phi \qquad (2)$$

Radiation losses | Ohmic heating

Energetic heating | Heat transfer between electrons and plasma ions

where K_e is the electron thermal conductivity and Z_a is the ionic charge.

The particle flux Γ_a is determined from the continuity equation

$$\frac{\partial n_a}{\partial t} = -\frac{1}{r}\frac{\partial (r\Gamma_a)}{\partial r} + \int S_{bc}\, dV\, \delta(a,b) + S_{ai} + S_{acx} \qquad (3)$$

Energetic ions transferred to plasma | Ionisation of neutrals | Charge exchange

and $$\Gamma_a = D_a \frac{\partial n_a}{\partial r} - R_a E_{tor} \qquad (4)$$

where D_a is the diffusion coefficient and the second term models the Ware pinch[12]; E_{tor} is the toroidal electric field.

The plasma neutrals are described by a Monte-Carlo code originally developed by Hughes and Post[13]. The neutral influx of atoms from the torus walls is composed of recycled plasma ions and neutrals from gas puffing. The recycling coefficient is set to 0.9 and the gas puffing rate is determined by the code from the requirement that the calculated plasma line average density is in agreement with experiment. There is a further source of neutrals from the injected beams. The plasma boundary condition is specified by fixed density and temperatures which remain constant for all plasma discharges.

Before neutral injection, the radiated power from the plasma is calculated from the impurity concentration n_z and a coronal equilibrium model[14]: the impurities are not allowed to diffuse. At the onset of neutral injection it is experimentally observed that the radiated power exhibits a rapid and often large increase which is at least partially due to the enhanced radiated power associated with charge exchange recombination of the injected energetic ions with the highly stripped plasma impurity ions. In the present paper the radiated power during injection has been modelled in one of two ways.

I. It is assumed that during injection the radiated power is enhanced by a factor γ over that given by the coronal equilibrium model. γ is chosen to give agreement with experiment. Although this model is rather arbitrary, it also represents a way of modelling impurity influx into the plasma. Experimentally it is apparent that the impurity concentration of the plasma sometimes rises during injection. Ideally, the impurity influx should be measured and provide an input

to the theoretical model. However, these measurements do not exist for the DITE discharges of Table 1.

II. The charge exchange recombination enhancement proposed by Hulse[15] is used.

In order to calculate the radiated power terms it is necessary to know the concentration of the various impurities (n_z/n_e) in the plasma. Although these can be obtained in principle from experimental spectroscopic data and then input to the code, for the discharges under consideration in this paper this information is generally not available. However, as experimental values of Z_{eff} and the radiated power $P_{rad}(r)$ are available, n_z/n_e is determined from this data, without injection, by assuming that only one species of heavy impurity (Fe) and one light impurity (O) is present. The Fe concentration is determined from the central value of the radiated power and the O concentration is then adjusted to give the correct Z_{eff}. This gives approximately the correct radiated power profile, although a further adjustment is made to n_{Fe} and n_O if there is a large discrepancy. The volume averaged radiated power is within a factor of 2 of the experimental value in the worst case. It is then assumed that these values of (n_z/n_e) are constant throughout the plasma and at all later times. It is realised that this procedure is not entirely satisfactory, but, in view of the experimental uncertainties, it is adequate for the present purposes.

The code was run with a radial mesh of 33 points and the points on the time mesh were separated by 0.5ms. Because the Monte-Carlo neutral package is the slowest part of this code it is run only every 15 time steps. This is not thought to lead to significant error in the present work. The calculations were all run on the CRAY 1 computer at NMFECC at Lawrence Livermore National Laboratory.

3. EXPERIMENTAL RESULTS

The DITE experiment[16] (R = 1.17m, a = 0.26m, B_ϕ < 2.7T) and its injection system[11] are shown schematically in Figure 1. All of the 1MW of neutral beam power is injected in the co-direction. The various diagnostics used are also shown in the figure. In Table 1 the main parameters of six different DITE discharges are shown. In addition, the time dependent variation of the plasma current (I_p), loop voltage (V_ℓ), line average density ($\bar{n}_e$), electron and ion temperature and radiated power are generally available together with the radial profiles of the latter four quantities. The ion temperature profiles are measured only as far as r = 0.18m and generally show a radial dependence of the form $T_i = T_{io}\ (1 - (r/a)^3)$. The electron density profiles are determined from the Abel inversion of a radial scan of the 2mm microwave system at low density and from the ruby laser Thompson scattering system at high density. The least accurate data was the radiated power (~ 40%).

It can be seen from Table 1 that a range of different injection heated discharges is covered with low density (A), low q (D), high density (D and E), low Z_{eff} (C and E). In all cases substantial ion heating is observed and in some cases (B, C and E) substantial electron heating also.

In addition the plasma neutral density (n_o) is estimated using a variety of techniques, but not necessarily for the discharges of Table 1. The methods are as follows:

i) The intensity of the signal observed by an absolutely calibrated[17] neutral particle analyser is proportional to an averaged value of $n_o n_e$. As n_e is known from the microwave diagnostic,

n_o can be determined.

ii) The shape of the spectrum of the fast injected ions as measured by the tangential neutral particle analyser is sensitive to the ratio of the fast ion slowing down time and charge exchange time. The former can be readily calculated from n_e and T_e; the latter is inversely proportional to n_o, allowing its determination.

iii) Measurement and Abel inversion of the intensity of H_α radiation gives a direct determination of n_o.

iv) If neoclassical effects are ignored, the ion density is determined by the equation

$$\frac{\partial n_i}{\partial t} = - \frac{1}{r} \frac{\partial}{\partial r} \left\{ r \, D_i \, \frac{\partial n_i}{\partial r} \right\} + n_e n_o \, \langle \sigma v \rangle_i \qquad (5)$$

In discharges in which n_i is rapidly increasing, the diffusion term is small and its neglect allows the determination of n_o assuming $n_i = n_e$. This is not a very satisfactory method because (a) it would be expected that the neutral density in this class of discharges would be large and (b) the lowest values of n_o obtained (see Figure 2) correspond to discharges with low values of $\partial n_i / \partial t$ in which diffusion effects are probably important.

v) A similar method to (iv) is used to obtain n_o in discharges in which the density exhibits sawtooth oscillations.

From Figure 2 it is seen that the values obtained from these quite different methods are very roughly in agreement with each other. n_o clearly decreases very rapidly with electron density. The values of n_o given by the curve as appropriate for discharges A to F will be adopted but it must be remembered that the values will be of no great accuracy.

4.1 INITIAL CHOICE OF TRANSPORT COEFFICIENT

For this study the transport coefficients are determined empirically and their initial values are determined as follows.

i) Electron thermal conductivity

If it is assumed that the electron energy containment time (τ_e) is determined entirely by electron conduction losses, then the following simple power balance determines K_e from the energy containment time and plasma energy (W_e)

$$\frac{W_e}{\tau_e} = K_e n_e \frac{\partial T_e}{\partial r} 2\pi R \, 2\pi a \qquad (6)$$

where τ_e is determined from a scaling law. If Alcator scaling[18] ($\tau_e = 4.0 \times 10^{-19} \bar{n}_e a^2$ s) is used then K_e is determined as $K_e = 7.5 \times 10^{17}/n_e$ cm^2 s^{-1} with n_e in units of cm^{-3}. The modified Alcator scaling[19] which includes a dependence on the plasma major radius gives $K_e = 3.4 \times 10^{17}/n_e$ for DITE. Our initial choice is therefore $K_e = 5 \times 10^{17}/n_e$ cm^2 s^{-1}.

ii) Ion thermal conductivity

Although several studies have shown that the experimental data in some machines is consistent with neoclassical ion heat conduction, a previous analysis[20] of a high power injection heated discharge in DITE showed that the ion thermal conductivity exceeded the neoclassical value by a factor of about 5, giving $K_i = 5 \times K_i$(Neoclassical).

The value used for K_i (Neoclassical) is as follows:

$$K_i(\text{Neoclassical}) = K_i(\text{plateau}) \quad \frac{0.36\nu_i^*}{1 + 0.36\nu_i^*} \tag{7}$$

with $$K_i(\text{Plateau}) = \frac{3}{2}\sqrt{\frac{\pi}{2}}\,\frac{v_i\, q\, \rho_{i\phi}^2}{R} \tag{8}$$

and collisionality parameter $$\nu_i^* = \left(\frac{R}{r}\right)^{3/2} \frac{q\, R}{v_i\, \tau_i} \tag{9}$$

where q is the plasma safety factor, v_i is the ion velocity, $\rho_{i\phi}$ is the ion Larmor radius in the toroidal field and τ_i is the ion collision time. These are defined as

$$v_i = \sqrt{\frac{T_i}{m_i}} \qquad \rho_{i\phi} = \frac{c\sqrt{2T_i m_i}}{Z_i\, e\, B\phi} \tag{10}$$

$$\tau_i = \frac{3m_i^{1/2}\, T_i^{3/2}}{4\pi^{1/2}\, n_i\, Z_i^4\, e^4\, \ln \Lambda} \tag{11}$$

where m_i is the ion mass and ln Λ is the Coulomb logarithm. Both plateau and neoclassical ion thermal conductivities together with ν_i^* are evaluated for the DITE discharges at r/a = 0.5 and are shown in Table 2. Our value of K_i (neoclassical) is between the values of refs[21,22] for the cases considered in this paper.

iii) Diffusion coefficient

Previous experimental data[9] suggests that the particle diffusion coefficient can be up to a factor of ten less than K_e. Alternatively, a simple model can be used to derive D from the neutral density data of Figure 2. If $\partial n/\partial t = 0$ and $S_{bc} = S_{acx} = 0$, equation 3 gives

$$r\,D\,\frac{\partial n}{\partial r} = -\int n_e n_o \langle \sigma v \rangle_i\, r\, dr \qquad (12)$$

If the quantities on the rhs are replaced by average values and the equation is evaluated over the central region of the plasma ($r/a \leq 0.5$), then $D = 2 \times 10^{16}/n_e$ (where $n_o = 1.6 \times 10^{22}/n_e$ has been used). The initial value chosen is therefore $1.6 \times 10^{16}/n_e$ with n_e in units of cm^{-3}.

4.2 SIMULATION RESULTS

The initially chosen set of transport coefficients gives results in reasonable agreement with experiment. However, the calculated electron temperatures both before and during injection are too low and K_e is therefore decreased to $2 \times 10^{17}/n_e$ to give better agreement.

The calculated ion temperatures during injection are initially too high and are therefore reduced by increasing the ion conductivity enhancement factor to 10. Although this produces an improved agreement, the central ion temperature is rather insensitive to this factor. Even after this change, the calculated ion temperature for discharge 'A' during injection is still too large and the calculated neutral density too small. In addition, the electron density profiles are too peaked during neutral injection. Because discharge 'A' is the lowest density discharge considered, both of these problems are overcome by using the modified diffusion coefficient below.

The final set of transport coefficients chosen are:

$$K_e = 2 \times 10^{17}/n_e \ cm^2\ s^{-1}$$

$$K_i = 10 \times K_i \ \text{(neoclassical)} \qquad (13)$$

$$D = \left\{3.9 \times 10^8 + \frac{2.7 \times 10^{22}}{n_e}\right\} \frac{1}{\bar{n}_e 0.43} \ cm^2\ s^{-1}$$

where $\bar{n}_e$ is the line averaged electron density. The diffusion coefficient at low and high densities is then:

(i) Low

$$\bar{n}_e = 2 \times 10^{13} \text{ cm}^{-3}$$

$$D = \left(740 + \frac{5.1 \times 10^{16}}{n_e}\right) \text{ cm}^2 \text{ s}^{-1} \qquad (14)$$

(ii) High

$$\bar{n}_e = 6 \times 10^{13} \text{ cm}^{-3}$$

$$D = \left(461 + \frac{3.2 \times 10^{16}}{n_e}\right) \text{ cm}^2 \text{ s}^{-1} \qquad (15)$$

In the initial calculations, radiation model I gives the results shown in Table 3. It is seen that, with the exception of discharge F before injection, where the calculated averaged $\langle T_e \rangle$ exceeds experiment by 60%, very good overall agreement is achieved for the temperatures both before and during injection. The total radiated power $\langle P_{rad} \rangle$ is in poorer agreement but, because of the large experimental errors on P_{rad}, there is little to be gained at present in trying to model these quantities more accurately.

The ion temperatures, while in reasonable overall agreement, show two systematic effects. (i) During injection, for the low density discharges T_i^{calc} exceeds T_i^{exp} with the opposite occurring in high density discharges. (ii) Before injection the calculated values of T_i are systematically too low. In fact, the ion temperatures before injection are best simulated with an ion conductivity enhancement factor of 4.

Despite the various uncertainties, the values obtained in Table 3 represent the best overall agreement which can be achieved without making many very detailed changes in the transport coefficients intended to improve the agreement in specific cases. We do not believe that this would produce an overall improvement in our ability to model other DITE discharges.

Some of the typical profiles are shown in Figures 3-6. In general, $n_e(r)$ is in good agreement with calculation for all discharges and it is interesting that for discharge F (Figure 3) the changes in profile before, during and after injection are well modelled. The shape of the electron temperature profile is also in good agreement (Figure 4). The experimental data on the ion temperature profiles is somewhat inadequate because measurements of T_i are generally available only out to r = 18cm. The profiles are very flat, varying typically as $[1 - (r/a)^3]$. In the example shown (Figure 5) the shape of $T_i(r)$ is well reproduced although the calculated magnitude of T_i is slightly too large.

A typical radial dependence of the radiated power is shown in Figure 6 before and during injection. The central peak in the calculated curve is caused by radiation from Fe whereas the peak at $r \approx 20$cm is caused by radiation from O. In the experimental curves this structure is eliminated, presumably because of contributions from impurities other than Fe or O.

Finally, in Figure 7, the comparison is made for the neutral density. The full line represents the average of the experimental values and the simulated values of n_o at r = 0 and 18cm are shown. The agreement at r = 0 is superficially excellent but it must be remembered that the experimental values probably represent averages over the central volume of the plasma.

The importance of the radiated power and the accuracy of the modelling is checked by comparing simulations with radiation models I and II, all other things equal. In Table 4 the electron temperature and total radiated power are shown for the two models for discharges A to F. Except for case A, the electron temperature does not vary greatly. It is clear that for discharge A the very large radiated power during injection effectively keeps T_e down at a low level. For discharges D and F the radiated power is adequately simulated by both models but for discharges A and B the large differences between models I and II imply an influx into the discharge during injection of impurities and this is not modelled in the present calculation. This is confirmed in an approximate way for discharge B by the rising plasma loop voltage during neutral injection at a time when T_e is also rising. Discharge C presents further difficulties because of the apparent very large observed rise of radiation at the onset of neutral injection. This seems to have been caused by experimental uncertainties and therefore and comparison has not been made in this case.

4.3 COLLAPSE OF DISCHARGE D

In discharge D the electron density increases to very nearly the disruptive limit. The behaviour of the simulation as this limit is approached is therefore of particular interest. The time dependence of $\bar{n}_e$ and central values of T_i and T_e are all shown in Figure 8. From the simulation it is clear that a collapse of T_e and T_i starts when the electron density reaches $\sim 4 \times 10^{13}$ cm^{-3} at 140 ms. This is caused by the dominance in the power balance of radiation (see Fig. 9) and ion losses which both increase further as the density increases,

causing the discharge to be extinguished in the simulation and leading to a disruption in the experiment. It is unfortunate that more detailed measurements of T_e do not exist; the ones shown, although in agreement with the simulation, are unable to confirm the detailed downward trend at $t > 150$ ms. However, the general shape of $T_i(t)$ is in good agreement with the simulation. This behaviour was not observed for the rather similar discharge 'E' because of the lower Z_{eff} and reduced role of radiation.

4.4 FUTURE NEUTRAL INJECTION ON DITE

At present the DITE neutral injection system is being modified to add two further injection lines and this will then give a total power to the plasma of 2.5 MW. It is therefore interesting to use the present set of transport coefficients to predict the plasma behaviour at this new power level. The radiation model I is used and it is assumed that, during injection, the radiated power is increased in proportion to power. The time dependent simulation runs at high and low injection power are shown in Figure 10 for discharges C and E.

For discharge C, the electron density rises rapidly because of beam refuelling. T_e increases only slightly compared with the 1.1 MW case, but T_i is approximately doubled at 1.35 keV. For discharge E the relative increase in injection power is much larger and substantially greater ion and electron heating is observed with maximum values of T_e = 1.45 keV and T_i = 1.45 keV. For the P_{NI} = 0.7 MW case, the droop in the $T_e(t)$ curve shows that the electron temperature is being depressed by the radiation loss which, in our model, increases with increasing density. Clearly the additional power overcomes this barrier.

5. SUMMARY AND CONCLUSIONS

(i) A wide range of injection heated discharges in DITE has been simulated with electron thermal conductivity $K_e = 2 \times 10^{17}/n_e$ and ion thermal conductivity 4-10 times the neoclassical value. Reasonably good agreement is found between simulation and experiment.

(ii) The largest uncertainties in the calculations result from inadequate knowledge of the impurity concentrations and from the poorly determined plasma neutral density.

(iii) Predictions of the degree of heating are obtained for the next stage of injection heating in DITE.

ACKNOWLEDGEMENT

We thank the DITE team for providing the experimental information. We also thank Dr. J. Killeen for his interest in and encouragement of this work.

TABLE 1

	A	B	C	D	E	F
B_ϕ (kG)	20	20	22	13.5	13.5	20
I_G (kA)	150	160	100	160	110	150
V_ℓ (v)	3.8	1.6	1.8	1.6	1.3	1.2
Z_{eff}	3.9	1.4	1.1	2.0	1.0	1.6
T_e (eV)	500	650	650	700	450	800
T_e' (eV)	500	1200	900	800	800	1050
T_i (eV)	300	210	220	200	190	250
T_i' (eV)	760	400	650	600	410	590
$\bar{n}_e$	1.2	3.4	1.6	1.0	3.3	2.8
$\bar{n}_e'$ (x 10^{13})	1.6	4.6	2.2	6.0	6.3	3.6
P_{NI} (MW)	0.9	0.8	1.1	0.62	0.68	1.0
Gas	H	D	D	D	D	D

Table with main experimental parameters for discharges A-F. The two entries for some parameters (eg. T_e, T_e') are the values before and during neutral injection. The temperatures all correspond to r = 0.

TABLE 2

Discharge	ν_i^*	K_i (plateau) (cm s^{-1})	K_i (NC) (cm^2 s^{-1})
A before NI	0.63	8.1×10^3	1.5×10^3
during NI	0.13	3.3×10^4	1.5×10^3
B	3.44	6.4×10^3	3.5×10^3
	1.32	1.6×10^4	5.3×10^3
C	2.62	1.0×10^4	4.9×10^3
	0.48	4.5×10^4	6.7×10^3
D	0.75	8.6×10^3	1.8×10^3
	0.49	4.5×10^4	6.7×10^3
E	4.55	1.1×10^4	6.8×10^3
	1.67	3.8×10^4	1.4×10^4
F	2.11	8.7×10^3	3.8×10^3
	0.48	3.2×10^4	4.7×10^3

TABLE 3

SUMMARY OF SIMULATION RESULTS

Discharge		$\langle T_e \rangle$ (eV)	$\langle T'_e \rangle$ (eV)	T_i (eV)	T'_i (kW)	$\langle P_{rad} \rangle$ (kW)	$\langle P'_{rad} \rangle$ (kW)	P_Ω (kW)
A	Exp	253	265	300	760	142	392	570
	Theory	276	274	200	980	72	540	
B	Exp	225	318	210	395	73	298	256
	Theory	188	355	200	480	120	198	
C	Exp	116	215	220	600	29	310	180
	Theory	144	353	130	810	21	168	
D	Exp	289	313	~200	600	-	279	256
	Theory	306	299	120	440	-	291	
E	Exp	132	249	180	410	-	-	143
	Theory	119	270	130	380	-	-	
F	Exp	265	317	250	590	94	251	180
	Theory	160	281	200	740	97	125	
Mean difference %		21	9	40	21	40	53	
Mean ratio		1.11	0.93	1.42	0.93	1.23	1.40	

Values of T_e, T_i etc. are those before (unprimed) and during (primed) neutral injection.

P_Ω is determined before injection.

$\langle T_e \rangle = \int T_e r dr / \int r dr$. T_i is the value at r = 0.

TABLE 4

Model	T_e			Radiated Power		
	I	II	Exp	I	II	Exp
Discharge						
A	550	1300	500	540	189	392
B	1200	1300	1200	198	50	298
D	1100	1100	800	291	265	279
E	900	900	800	-	-	-
F	1200	1200	1050	125	129	251

Electron temperature and radiated power for the different radiation models during neutral injection.

REFERENCES

1) D.F. Düchs, H.P. Furth and P.H. Rutherford. Plasma Physics and Controlled Nuclear Fusion Research, 1971 (Madison), 1 (1972) 411. IAEA, Vienna.

2) D.F. Düchs, H.P. Furth and P.H. Rutherford. 5th European Conf. on Controlled Fusion and Plasma Physics, (Grenoble), 1 (1972) 14.

3) D.F. Düchs, D.E. Post and P.H. Rutherford. Nuclear Fusion, 17 (1977) 565.

4) J. Killeen et al. Modern Plasma Physics. (Trieste Course, (1979)), (1981) 395, IAEA, Vienna.

5) A.A. Mirin et al. J. Comp. Phys. 23 (1977) 23.

6) A.A. Mirin et al., Proc. of Plasma Heating in Toroidal Devices, (Grenoble), 1 (1978) 13.

7) A.A. Mirin and D.J. Jassby. IEEE Transactions on Plasma Science, PS-8, No. 4 (1980) 503.

8) A.A. Mirin and D.J. Jassby. LLNL Report UCRL-85119 (1980).

9) J. Hugill. Nuclear Fusion, to be published.

10) G.G. Lister et al. Proc. of Plasma Heating in Toroidal Devices, (Varenna), 1 (1976) 303.

11) R.S. Hemsworth et al. Heating in Toroidal Plasmas, (Grenoble), ed. T. Consoli 1 (1979) 83. (Pergamon Press, Oxford)

12) J.W. Connor. Plasma Physics, 15 (1973) 765.

13) M.H. Hughes and D.E. Post. J. Comp. Phys., 28 (1978) 43.

14) D.E. Post et al. Atomic Data and Nuclear Tables, 20 (1977) 397.

15) R.A. Hulse, D.E. Post and D.R. Mikkelson. J. Phys. B, 13 (1980) 3895.

16) J.W.M. Paul et al. Plasma Physics and Controlled Nuclear Fusion Research, (Berchtesgaden), 2 (1977) 269. IAEA, Vienna.

17) D.D.R. Summers, R.D. Gill and P.E. Stott. J. Phys. E., 11 (1978) 1183.

18) E. Agpar et al. Plasma Physics and Controlled Nuclear Fusion Research, (Berchtesgaden, 1 (1977), 247. IAEA, Vienna.

19) W. Pfeiffer and R.E. Waltz. Nuclear Fusion, 19 (1979) 51.

20) R.D. Gill, Proc. of 9th Euro. Conf. on Controlled Fusion and Plasma Physics, 1979, paper EP9.

21) F.L. Hinton and R.D. Hazeltine. Rev. Mod. Phys., 48 (1976) 239.

22) F.L. Hinton and M.N. Rosenbluth. Phys. Fluids, 16 (1973) 836.

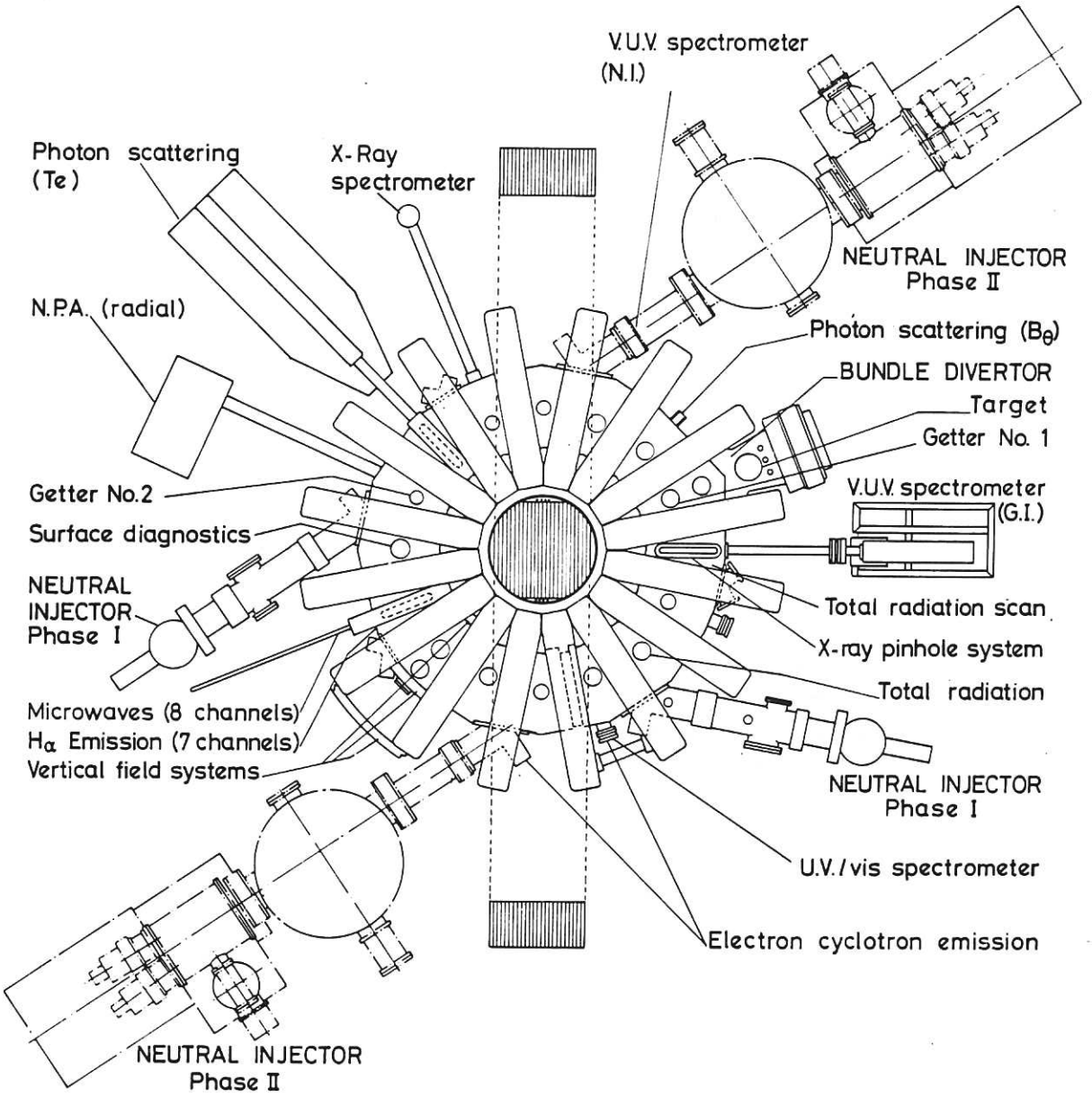

Fig.1 Schematic of DITE and the 1 MW neutral injection system.

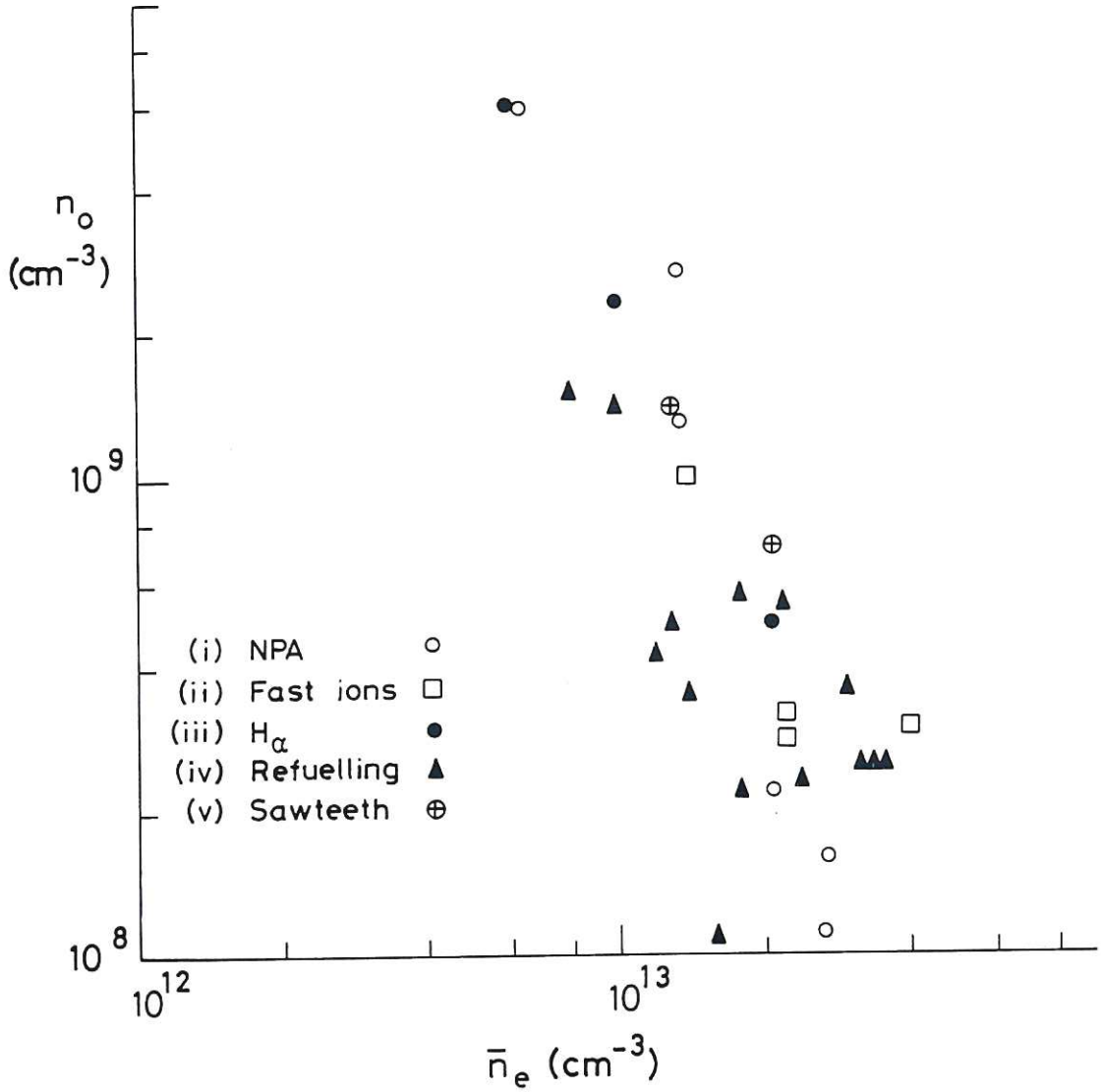

Fig.2 Plasma neutral density determined by five different methods.

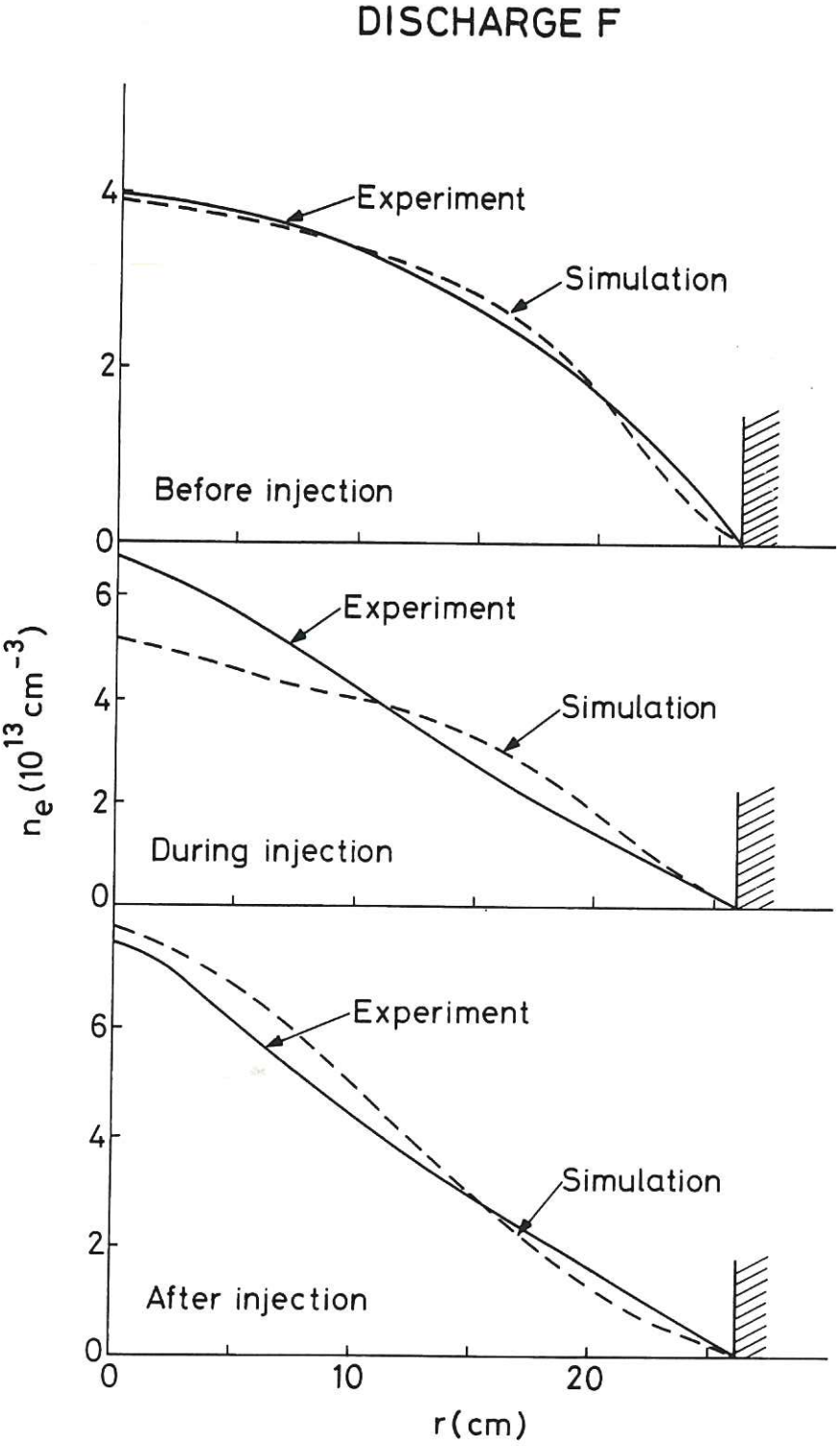

Fig.3 Electron density radial profiles before, during and after neutral injection for discharge F.

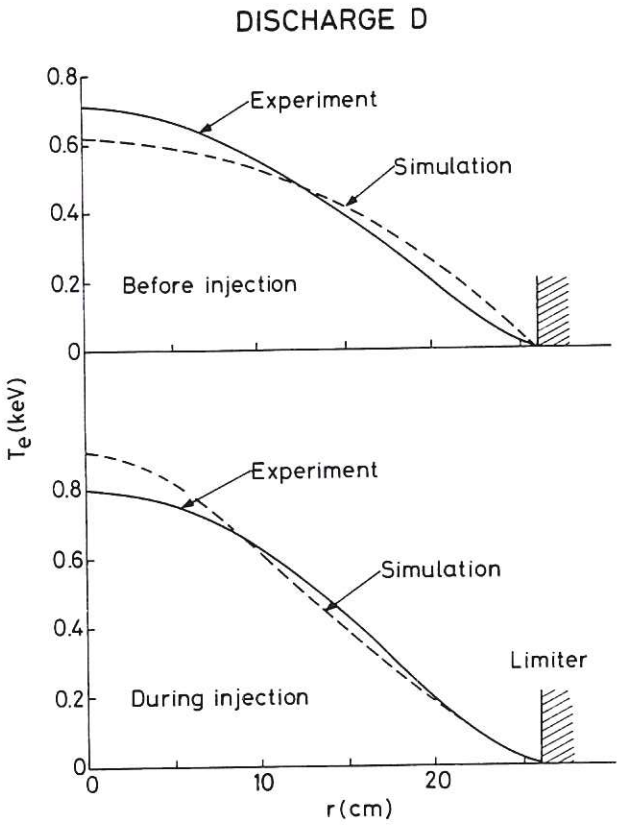

Fig.4 Electron temperature profiles before and during injection for discharge D.

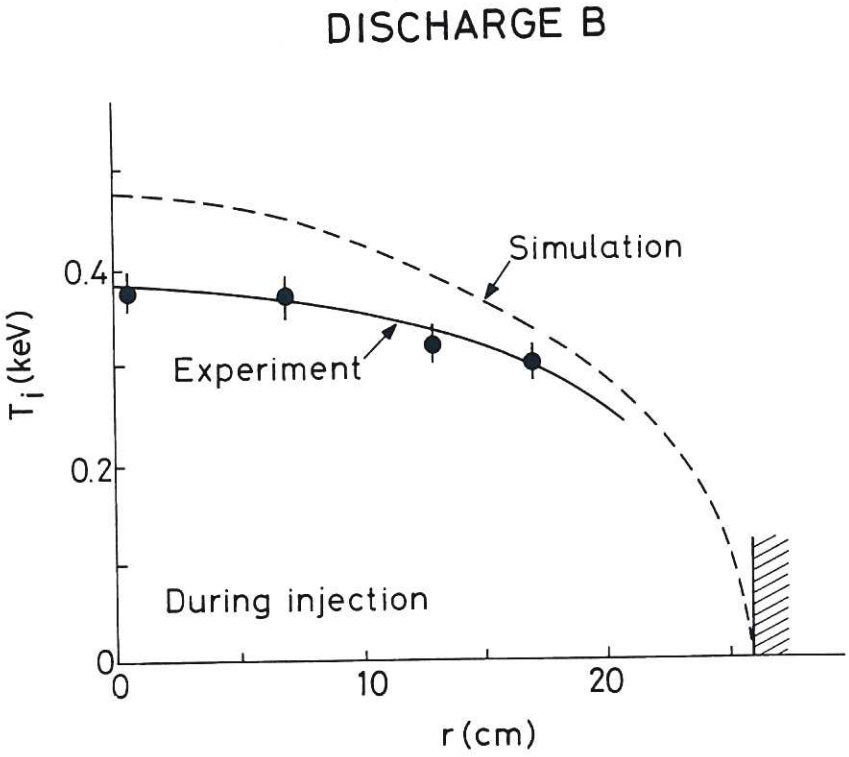

Fig.5 Ion temperature profile for discharge B.

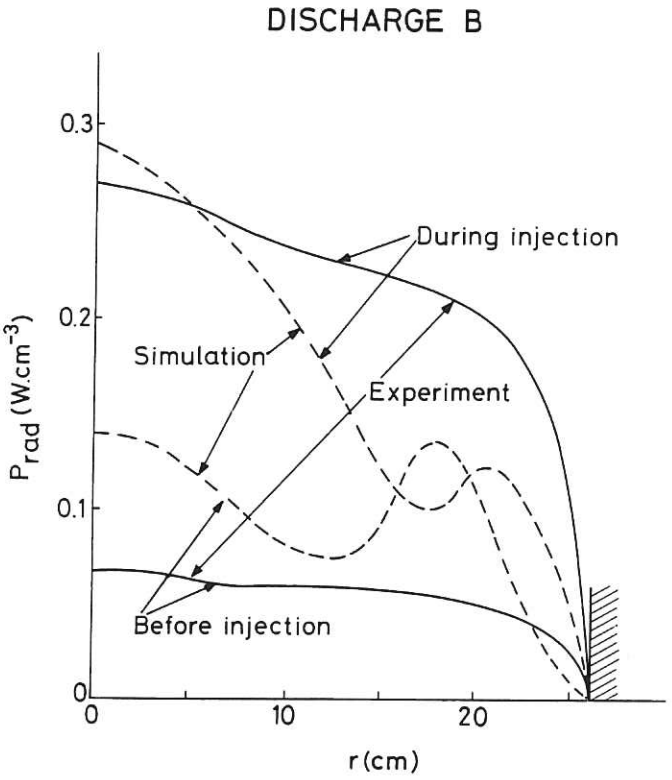

Fig.6 Radiated power profiles before and during injection for discharge B.

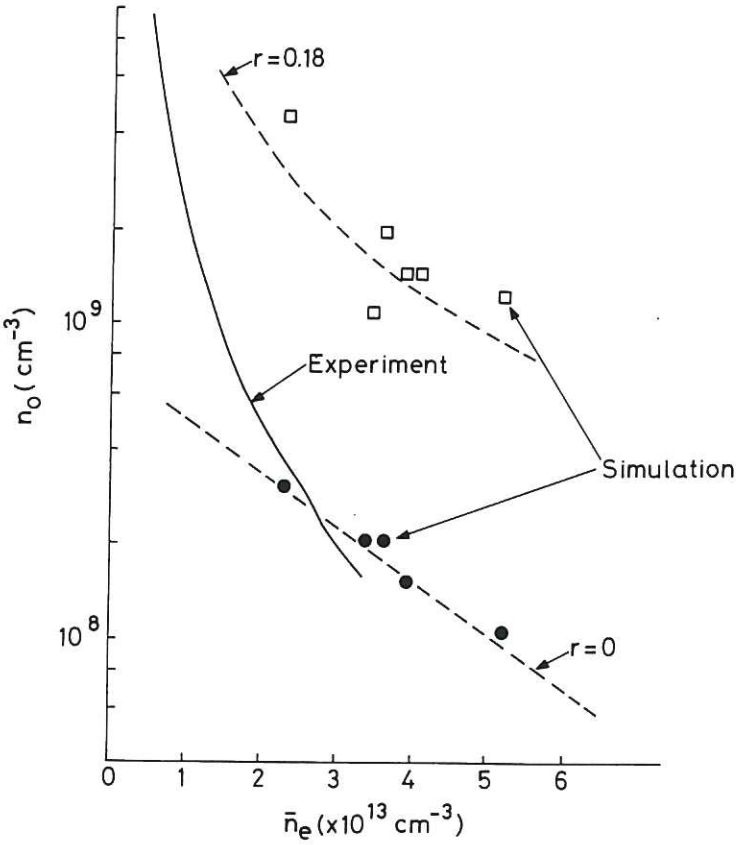

Fig.7 Simulated and experimental neutral density for D_2 discharges.

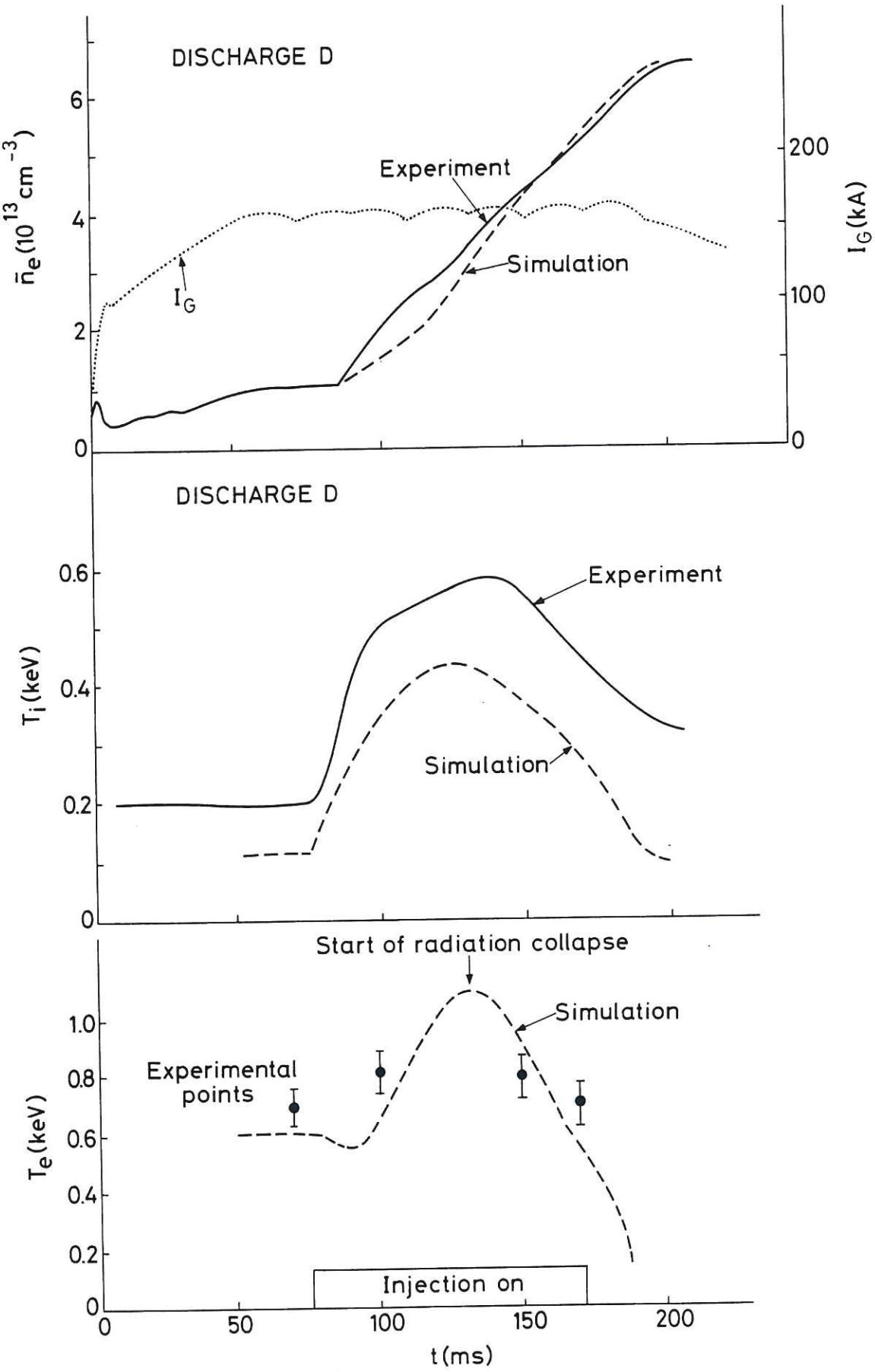

Fig.8 Simulation of the radiation collapse of discharge D.

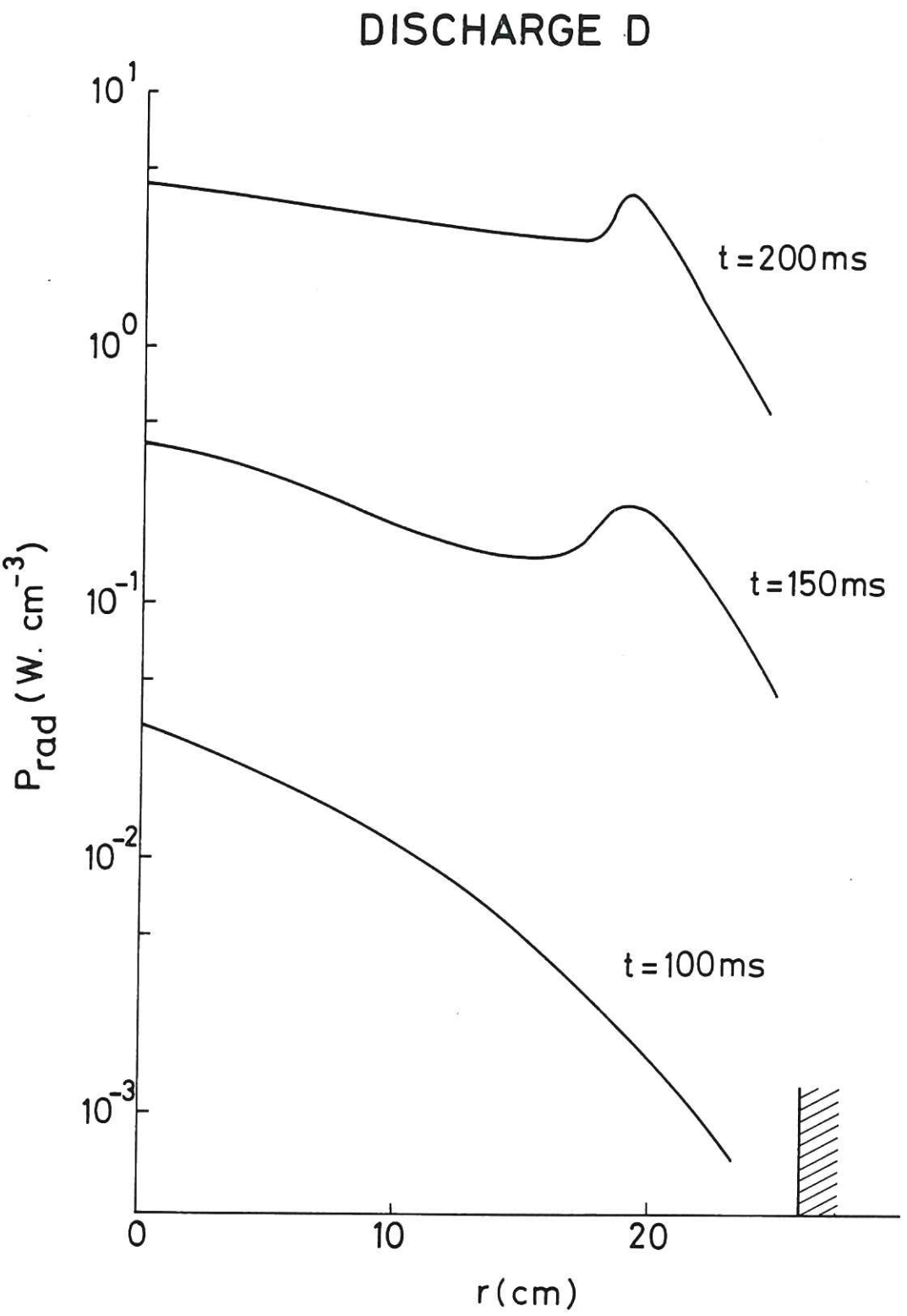

Fig.9 Radiated power profiles at various times during discharge D.

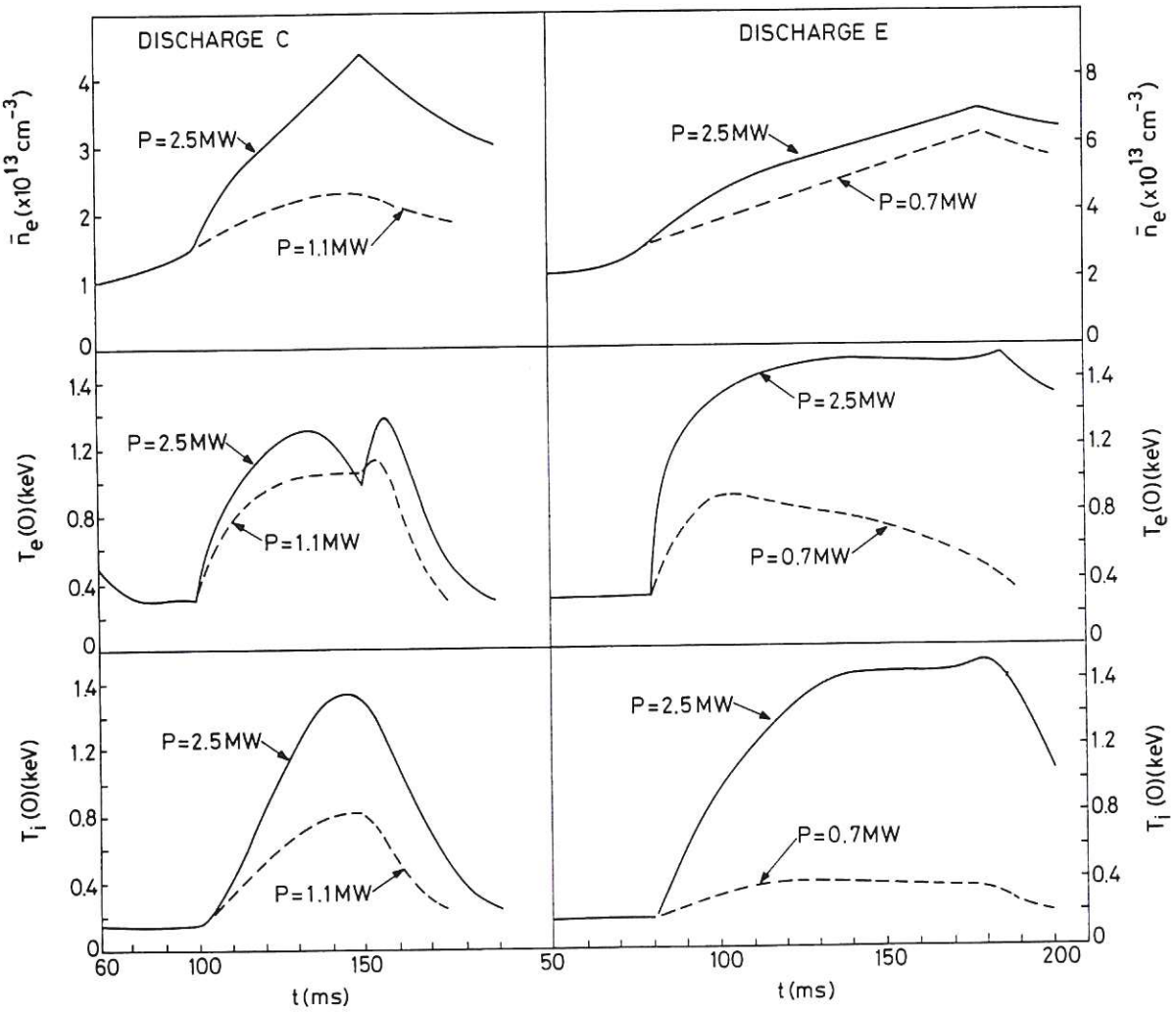

Fig.10 Effects of increasing the total injection power to 2.5MW.